Resting GABA and glutamate concentrations do not predict visual gamma frequency or amplitude

Helena Cousijn[a,b,1], Saskia Haegens[c,d], George Wallis[b], Jamie Near[e], Mark G. Stokes[b], Paul J. Harrison[a], and Anna C. Nobre[b]

[a]Department of Psychiatry and [b]Oxford Centre for Human Brain Activity, Warneford Hospital, University of Oxford, Oxford OX3 7JX, United Kingdom; [c]Department of Psychiatry, Columbia University College of Physicians and Surgeons, New York, NY 10032; [d]Cognitive Neuroscience and Schizophrenia Program, Nathan Kline Institute, Orangeburg, NY 10962; and [e]Douglas Mental Health University Institute and Department of Psychiatry, McGill University, Montreal, Canada H4H 1R3

Edited by Leslie G. Ungerleider, National Institute of Mental Health, Bethesda, MD, and approved May 8, 2014 (received for review November 11, 2013)

Gamma band oscillations arise in neuronal networks of interconnected GABAergic interneurons and excitatory pyramidal cells. A previous study found a correlation between visual gamma peak frequency, as measured with magnetoencephalography, and resting GABA levels, as measured with magnetic resonance spectroscopy (MRS), in 12 healthy volunteers. If true, this would allow studies in clinical populations testing modulation of this relationship, but this finding has not been replicated. We addressed this important question by measuring gamma oscillations and GABA, as well as glutamate, in 50 healthy volunteers. Visual gamma activity was evoked using an established gratings paradigm, and we applied a beamformer spatial filtering technique to extract source-reconstructed gamma peak frequency and amplitude from the occipital lobe. We determined gamma peak frequency and amplitude from the location with maximal activation and from the location of the MRS voxel to assess the relationship of GABA with gamma. Gamma peak frequency was estimated from the highest value of the raw spectra and by a Gaussian fit to the spectra. MRS data were acquired from occipital cortex. We did not replicate the previously found correlation between gamma peak frequency and GABA concentration. Calculation of a Bayes factor provided strong evidence in favor of the null hypothesis. We also did not find a correlation between gamma activity and glutamate or between gamma and the ratio of GABA/glutamate. Our results suggest that cortical gamma oscillations do not have a consistent, demonstrable relationship to excitatory/inhibitory network activity as proxied by MRS measurements of GABA and glutamate.

Gamma band oscillations (30–90 Hz) are found in many cortical areas and are thought to play an important role in cognitive processing (1). Both experimental and modeling studies have shown that the gamma rhythm is inextricably linked to synaptic inhibition (2–4). GABA-mediated inhibition is both necessary and sufficient for the generation of gamma oscillations, and mutually connected inhibitory interneuron networks are major generators of gamma oscillations (4–6). In addition, fast recurrent excitation followed by slower feedback inhibitions can give rise to gamma oscillations (3, 7). Most likely, excitation–inhibition and inhibition–inhibition hybrid gamma networks work together to generate gamma frequency oscillations (2, 8).

In vitro and modeling studies have clearly shown the importance of GABA for the generation of gamma oscillations, but the relationship between GABA and gamma is not easily assessed in the human brain. Muthukumaraswamy and colleagues (9) attempted to assess this relationship by correlating resting GABA concentrations as measured by magnetic resonance spectroscopy (MRS) with visual gamma oscillations as measured by magnetoencephalography (MEG). MRS provides a noninvasive method of quantifying metabolite concentrations in discrete regions of the human brain, but it can only detect the total concentration of a neurochemical and cannot distinguish between separate functional pools (10). In their study, Muthukumaraswamy and colleagues (9) found a correlation between resting GABA levels and visual gamma peak frequency in 12 participants. GABA levels in individuals correlated with the frequency level displaying the greatest power within the gamma band (gamma peak frequency). The correlation was speculated to reflect a dependence of gamma oscillations on GABA concentrations, as measured by MRS, with these GABA concentrations providing a window into pyramidal-interneuron network properties. If true, such a correlation would make gamma peak frequency a useful surrogate marker of cortical excitability for studies investigating clinical populations and/or the effects of pharmacological agents. Furthermore, this finding would have implications for the interpretation of MEG experiments because differences in gamma oscillations might actually be explained by differences in GABA, independent of the paradigm used. The same group later reported a similar correlation in a sample of 13 participants, seven of whom participated in both studies (11). Gaetz and colleagues (12) observed a correlation between GABA and gamma frequency in the motor cortex of nine healthy adults. However, no independent replications of these important results in the visual system have been published to date.

In this study, we addressed the question of whether resting GABA concentrations as measured by MRS correlate with the peak frequency of visual gamma oscillations in a much larger sample than hitherto. In 50 healthy volunteers, we measured concentrations of endogenous resting GABA from a voxel in the occipital cortex, using MRS, and stimulus-induced gamma

Significance

In vitro and modeling studies have indicated that GABAergic signaling underlies gamma oscillations. It would be valuable to measure this correlation between GABA and gamma oscillations in the human brain, and a recent study [Muthukumaraswamy SD, et al. (2009) *Proc Natl Acad Sci USA* 106(20):8356–8361] indicated that this is possible, using magnetoencephalography and magnetic resonance spectroscopy. If true, such a correlation would make the gamma peak frequency a useful surrogate marker of cortical excitability for studies investigating clinical populations and/or the effects of pharmacological agents. However, magnetic resonance spectroscopy does not measure synaptic GABA specifically, and the results from the current study (n = 50) indicate that GABA, as measured with magnetic resonance spectroscopy, does not correlate with gamma peak frequency.

Author contributions: H.C., P.J.H., and A.C.N. designed research; H.C., G.W., and M.G.S. performed research; S.H. and J.N. contributed new reagents/analytic tools; H.C., S.H., and G.W. analyzed data; and H.C., P.J.H., and A.C.N. wrote the paper.

The authors declare no conflict of interest.

This article is a PNAS Direct Submission.

Freely available online through the PNAS open access option.

Data deposition: The data will be made available upon request.

[1]To whom correspondence should be addressed. E-mail: helenacousijn@gmail.com.

This article contains supporting information online at www.pnas.org/lookup/suppl/doi:10.1073/pnas.1321072111/-/DCSupplemental.

NEUROSCIENCE

oscillations in the occipital cortex, using MEG. Because of the proposed interplay between inhibition and excitation in the generation of gamma oscillations, we also measured glutamate concentrations and correlated these as well as the ratio of GABA/glutamate with gamma frequency and amplitude.

Results

For MR data acquisition, a 3T Siemens scanner was used. Sagittal and axial T1 scout images were acquired and used to place a $2 \times 2 \times 2$ cm^3 voxel of interest manually in the occipital cortex (Fig. 1). The spin-echo full-intensity acquired localized (SPECIAL) sequence, originally developed by Mlynárik and colleagues (13) and adapted for humans by Mekle and coworkers (14), was used for single-voxel spectroscopy measurements. The spectra were quantitatively analyzed, using a linear combination model. This model analyzes the in vivo spectrum as a linear combination of a basis set of simulated metabolite spectra (15) (Fig. 1). This way, GABA and glutamate estimates were obtained for all participants.

Gamma oscillations in the occipital cortex were induced by presenting vertical, stationary gratings of 3 cycles per degree at maximum contrast. Sensor space analysis showed a clear increase in visual gamma power (40–80 Hz) in posterior regions in response to these gratings (cluster-based randomization test $P < 0.05$; Fig. 2*A*). This increase in gamma band power was sustained for the duration of the stimulus (Fig. 2*B*). We applied a beamformer spatial filtering technique to extract source-reconstructed gamma peak frequency and amplitude from the occipital lobe. Individual participants showed clear gamma responses in visual regions (Fig. 2*C*), with the source space time–frequency representations also showing sustained gamma for the duration of the stimulus presentation (Fig. 2*D*). Fig. S1 shows the localization of the gamma peak for all participants. Fig. 3 indicates that responses to left gratings were lateralized to the right hemisphere, with responses to right gratings being lateralized to the left hemisphere.

For each individual participant, Fourier spectra for the gamma range (40–80 Hz) were obtained with fast Fourier transform (FFT), using Slepian multitapers (±5 Hz spectral smoothing) applied to 1-s data segments for the baseline time window (−1.0 to 0 s) and the time window of interest (0.5–1.5 s and 1.0–2.0 s stimulus presentation). We extracted the gamma peak frequency and amplitude from the voxel in occipital cortex where the power of gamma was largest, from the voxels in right/left occipital cortex where the power of gamma was largest (based on left gratings only and on right gratings only, respectively), and from the location of the MRS voxel. Spectra were plotted relative to baseline, and peak frequency and amplitude information was extracted. In addition to taking the highest value from the "raw" spectra, we also fitted Gaussian curves to the spectra to establish the existence of unambiguous peaks for all individual subjects. Representative spectra for individual participants can be seen in Fig. 2*E*.

Gamma peak frequency based on the raw spectra and gamma peak frequency based on the Gaussian fit showed a strong correlation of $r = 0.892$ ($P < 0.001$). To confirm the quality of the data and the reliability of the estimates, we estimated gamma peak frequencies for independent data from the left and right gratings, which were strongly correlated ($r = 0.714$; $P < 0.001$; Fig. 3), as were our estimates based on the peak activity region of interest and the MRS voxel region of interest ($r = 0.812$; $P < 0.001$). Having confirmed the quality of our measurements, we tested for the reported correlation between GABA and gamma peak frequency. We found no correlation between GABA and any of our gamma peak frequency measures [GABA − gamma based on peak activation: $r = -0.114$ ($P = 0.473$); GABA − gamma based on MRS voxel: $r = -0.064$ ($P = 0.687$); GABA − gamma based on

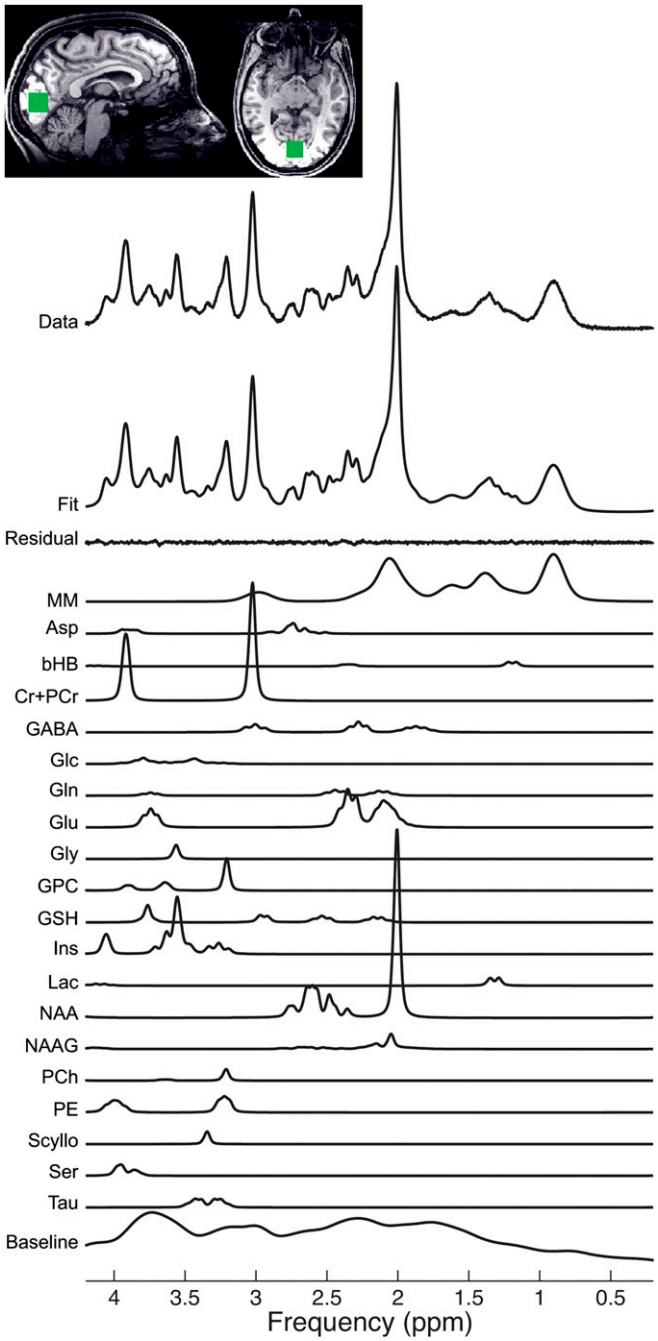

Fig. 1. A typical spectrum from the occipital voxel (placement depicted), acquired using the SPECIAL sequence. The original MRS data are shown in the top row. The next row is the model fit produced from a linear combination model (15). The high quality of the fit is demonstrated by the small residual remaining after fitting, shown by the row labeled "residual." Below, individual fits for all neurochemicals are demonstrated. Each neurochemical has multiple fitted peaks that reflect the individual protons within the molecule. Asp, aspartate; bHB, beta-hydroxybutyrate; Cr+PCr, total creatine; GABA, gamma-aminobutyric acid; Glc, glucose; Gln, glutamine; Glu, glutamate; Gly, glycine; GPC, glycerophosphocholine; GSH, glutathionine; Ins, myo-inositol; Lac, lactate; MM, macromolecules; NAA, n-acetylaspartate; NAAG, n-acetylaspartylglutamate; PCh, phosphocholine; PE, phosphorylethanolamine; Scyllo, scyllo-inositol; Ser, serine; Tau, taurine. GABA is found at a low concentration in the brain, as reflected by the relatively low-amplitude peaks. Despite this low concentration, the high quality of the fit for GABA is demonstrated by Cramer-Rao bands <20%.

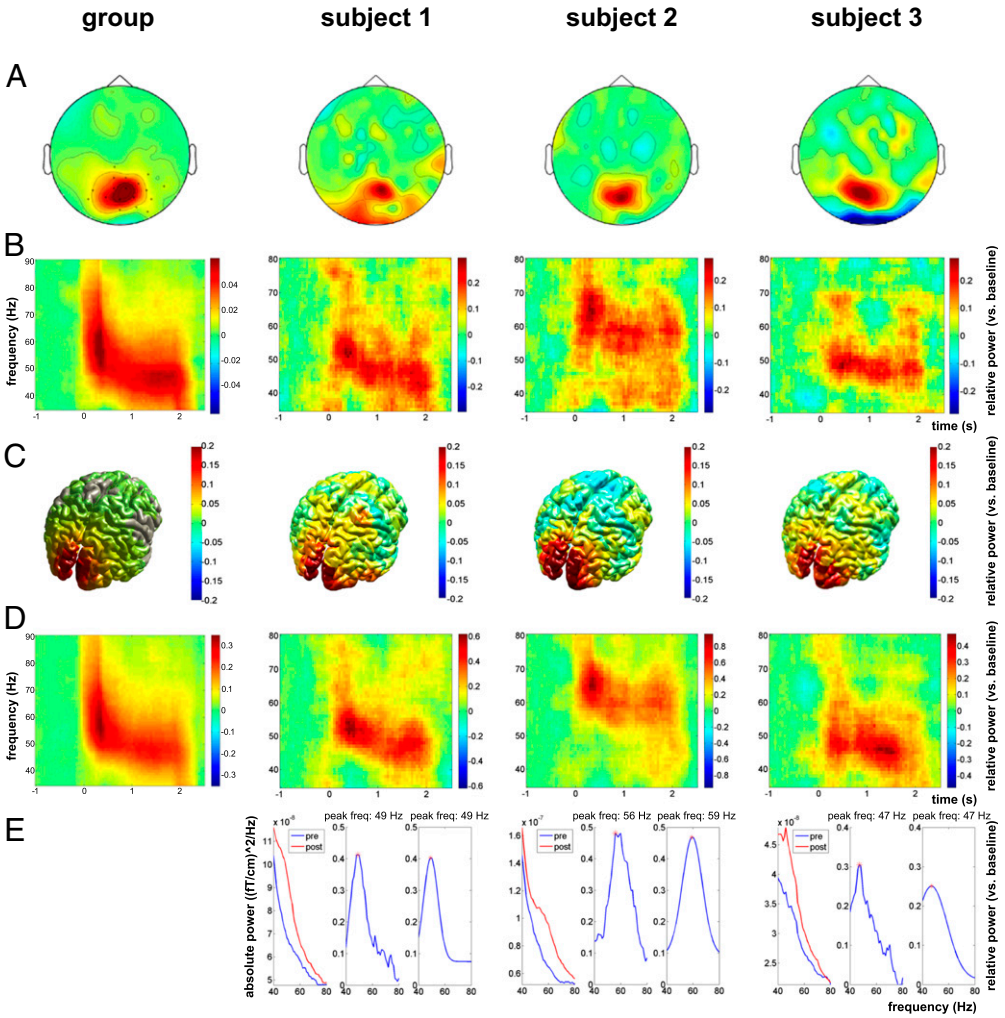

Fig. 2. Gamma band activation in response to presentation of the gratings at the group level and for three representative subjects. (*A*) Topoplots showing the location of activation in the gamma band at the sensor level. (*B*) Time-frequency representations show sustained activation in the gamma band for the duration of the stimulus presentation at posterior sensors. (*C*) Localization of gamma band activation in response to the gratings in source space. (*D*) Time-frequency representations show sustained activation at the location with peak activation in the gamma band. These patterns strongly resemble those in sensor space. (*E*) Graphs show the fitted peaks for each individual participant. The first part of the graph shows the spectrum before (blue) and during (red) the presentation of the grating (this is absolute power). The second graph shows the relative difference between these two spectra and the peak activation for the subject. The third graph shows the fitted Gaussian curve.

left stimulus: $r = -0.132$ ($P = 0.404$); GABA − gamma based on right stimulus: $r = -0.230$ ($P = 0.143$)] (Fig. 4).

In addition to Pearson's correlation coefficient, we calculated a Bayes factor (BF) based on the methods described by Wetzels and Wagenmakers (16). This BF summarizes the ratio of evidence for a correlation of any kind versus the evidence for the null hypothesis of no correlation. Even though there are no categorical boundaries, a BF <0.3 is seen as providing evidence in favor of the null hypothesis and a BF >3 as strong evidence against it (17). We found the BF to provide evidence in favor of the null hypothesis (GABA − gamma based on peak activation: BF = 0.156; GABA − gamma based on MRS voxel: BF = 0.131). In addition, no correlations were found between GABA and gamma amplitude ($r = 0.151$; $P = 0.341$) or between glutamate and gamma peak frequency ($r = -0.105$; $P = 0.509$), glutamate and gamma amplitude ($r = 0.120$; $P = 0.449$), GABA/glutamate and gamma peak frequency ($r = -0.055$; $P = 0.729$), or GABA/glutamate and gamma amplitude ($r = 0.060$; $P = 0.705$). Given that only men participated in the study reported by Muthukumaraswamy and colleagues (9), we also calculated the correlation between gamma peak frequency and GABA in men only but found no correlation in this group ($r = 0.239$; $P = 0.310$).

Discussion

The role gamma oscillations play in cognitive function, and their cellular and neurochemical basis, are both under active investigation. In this regard, a paper reporting that cortical gamma peak frequency correlated with GABA concentration generated considerable interest. We sought to replicate and extend this observation in a considerably larger study. However, we did not find any such relationship. As in previous studies (9, 11), we also did not find a correlation between resting GABA and gamma amplitude or between glutamate (or the GABA:glutamate ratio) and gamma activity.

To guard against a type 2 error and ensure the most optimal analysis of the datasets, the data were analyzed using several techniques. We initially attempted to assess the relationship between MRS GABA and gamma oscillations in a more direct way by taking both measurements from the same anatomical location. We also extracted frequency and amplitude from the

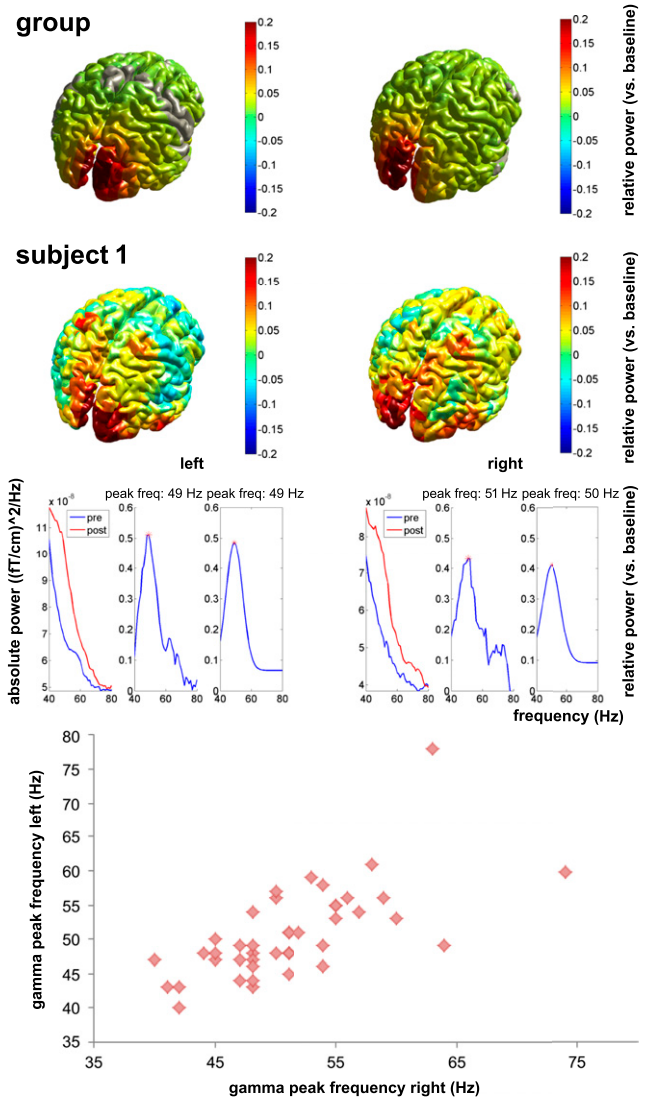

Fig. 3. The upper part of the figure shows that activations in the gamma band in response to the gratings are lateralized, with the presentation of gratings on the left side of the screen leading to activation in the right occipital lobe and presentation of gratings on the right side of the screen leading to activation in the left occipital lobe. The row below shows a similar lateralized activation pattern in a representative subject (subject 1). Underneath, the peak frequencies in the left and right occipital lobe are shown for this same subject. The lower part of the figure shows the strong correlation between gamma peak frequency estimates for the left and right gratings separately.

spatial peak of the activity for each individual participant so that our measures would be derived from the strongest gamma oscillations present. To make our study as comparable as possible with the study of Muthukumaraswamy and colleagues (9), we also analyzed the data based on the left gratings only. In addition to using the maximum value of the FFT spectra, we fitted a Gaussian curve to the spectra to assess peak frequency. This makes explicit the assumption that there is a peak and is less susceptive to incorrect detection of a spurious local maximum. All the different measures of gamma activity correlated significantly with each other, but none correlated with the measured GABA concentrations, together providing convincing evidence against such a correlation existing.

The reasons for the discrepancy between our results and those reported by Muthukumaraswamy and colleagues (9) are unclear. One difference is the type of MRS sequence used to acquire the data. Whereas the previous study used a spectral editing method (MEGA-PRESS), we used short-echo-time MRS (SPECIAL). The use of SPECIAL yields a factor two improvement in signal-to-noise ratio compared with MEGA-PRESS because of the shorter echo time and the fact that MEGA-PRESS has an editing efficiency of less than 40%. The SPECIAL technique also has the advantage that it detects all three methylene resonances of GABA and uses all of them to estimate its intensity, whereas the MEGA-PRESS technique only detects one of the methylene resonances (18). Furthermore, the difference in methodology will have led to differences in macromolecule contamination in the GABA measurements. MEGA-PRESS typically contains 50% macromolecule

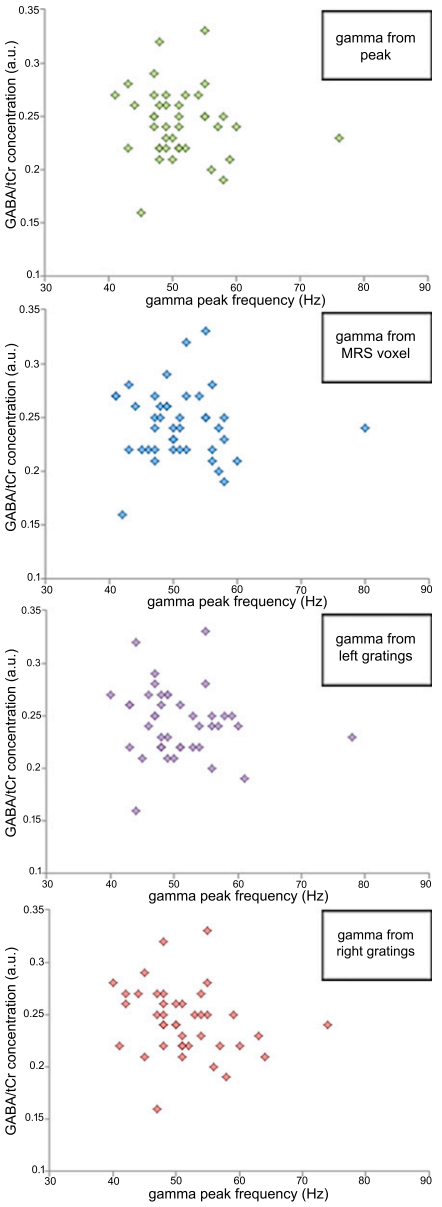

Fig. 4. No correlations were observed between GABA concentration and gamma peak frequency based on the peak activation (*Upper*), between GABA concentration and gamma peak frequency from the location of the MRS voxel (*Second image*), between GABA concentration and gamma peak frequency based on left gratings only (*Third image*), or between GABA concentration and gamma peak frequency based on right gratings only (*Bottom*). tCr = total creatine; $n = 42$.

contamination (18), whereas the SPECIAL sequence is less susceptible to macromolecule contamination (19). Although MEGA-PRESS is more commonly used, SPECIAL has been successfully used in several studies (20, 21), and it has been shown that short-TE measurements of GABA have good reproducibility and correspond well with measurements made using spectral editing techniques (19). We therefore feel that the different MRS methods used are unlikely to explain the discrepant findings.

Gamma oscillations are generated within complex networks of inhibitory GABAergic and excitatory glutamatergic cells, with recorded gamma waves largely corresponding to synchronous inhibitory postsynaptic potentials in pyramidal cells brought about by fast-spiking interneurons (2). Under basal conditions, the MRS GABA signal arises mostly or almost entirely from the large cytoplasmic GABA pool in GABAergic neurons, the functional significance of which is not known (22). Therefore, MRS GABA seems unlikely to reflect primarily the activity of GABAergic interneurons, including those within gamma-generating networks (10). Studies have tried to address this issue by correlating MRS GABA measures with TMS measures of synaptic GABA-A and GABA-B (20, 23) because different TMS protocols can be used to specifically assess GABA-A and GABA-B activity. No correlation between MRS GABA measures and TMS measures of synaptic GABA-A and GABA-B activity was found, supporting the view that MRS-derived GABA levels do not reflect specific synaptic activity.

Pharmacological MEG studies have also addressed the relationship between GABA and gamma oscillations in the human brain. Hall and colleagues (24) found that diazepam, which increases the effects of GABA, increases gamma power, but not gamma frequency, in the occipital cortex, whereas a similar study by Hall and coworkers (25) focusing on motor areas showed no such modulation. Muthukumaraswamy and colleagues (26) found that elevation of extracellular GABA levels by tiagabine, which blocks GABA reuptake, did not modulate gamma oscillations in either visual or motor cortex. Finally, Saxena and colleagues (27), using GABA-A agonist propofol, observed an increase in stimulus-induced gamma amplitude only. Taken together, none of these studies provides support for a measurable relationship between GABA levels and visual gamma frequency in the human brain.

We are convinced that our findings suggest a real lack of linear relation between resting GABA concentrations and gamma peak frequency. We used a substantially larger number of participants than previous studies and carried out several checks to ensure the quality of our data and analyses. However, it is always difficult to prove a null result using standard statistical methods. For this reason, we also applied the alternative approach of Bayesian statistics. Bayesian methods not only provide evidence against the null hypothesis but also weigh the evidence for H0 versus H1 for a given body of data (17). In our case, we found clear evidence in favor of the null hypothesis. When we calculated the same BF for the results of Muthukumaraswamy and colleagues (9), we found that their data do provide evidence of a correlation between gamma and GABA (BF = 4.12). However, a recent study (28) assessing GABA and gamma oscillations in participants with remitted depression ($n = 19$) and healthy controls ($n = 18$) also found no correlation between GABA and gamma, providing accumulating evidence in favor of the null hypothesis.

In sum, our results suggest that cortical gamma oscillations do not have a demonstrable relationship to excitatory/inhibitory network activity as proxied by MRS measurements of GABA and glutamate concentrations. Other methods may be needed to elucidate the relationship between gamma oscillations and GABA/glutamate in the human brain.

Methods

Participants and Stimuli. Fifty healthy right-handed volunteers (23 men, 27 women) ranging from 19–34 y old [mean age, 24 y (SD 4.11)] with normal or corrected-to-normal vision participated in this experiment. All participants reported no history of neurological or psychiatric disorders and were medication-free. Ethical approval was obtained from the National Health Service Berkshire research ethics committee, and all participants provided written informed consent. MEG and MRS data were acquired on separate days.

During the MEG session, stimuli consisting of vertical, stationary gratings of 3 cycles per degree and a diameter of 4° visual angle were presented at maximum contrast on a mean luminance, gray background using a Panasonic PT D7700E projector. Multiple studies have shown that the presentation of gratings is a reliable method to induce gamma responses (e.g., refs. 29–31). Gratings were presented for 2 s at a peripheral location within the lower left or right visual field (centered over 2.5° eccentricity) and always followed by 2 s of fixation without gratings present on the screen. Blocks of left or right visual field stimulation contained five stimuli followed by 20 s fixation during which the subjects were allowed to blink. Overall, 90 stimuli were presented. Participants were instructed to maintain fixation on a dot in the middle of the screen for the duration of the experiment.

MEG Methods. Whole-head MEG recordings were acquired using the Elekta NeuroMag MEG System. Data from the 204 gradiometers were analyzed. The signal was digitized at a sampling rate of 1,000 Hz, with a high-pass filter of 0.03 Hz and a low-pass filter of 330 Hz. A magnetic digitizer (Polhemus FastTrak 3D) was used to measure the relative positions of four head-position indicator coils and three anatomical landmarks (nasion and left and right auricular points). These coordinates were used for coregistration of the sensor montage to the participant's structural MRI scan.

The data were analyzed using the Matlab-based Fieldtrip toolbox (32) (www.ru.nl/neuroimaging/fieldtrip). Offline, data were low-pass filtered at 200 Hz and high-pass filtered at 0.5 Hz. Data were downsampled to 500 Hz. Bad channels and trials were rejected on visual inspection. We used independent component analysis (33) to identify eye artifacts, which were then projected out of the data. Line noise was removed using a bandstop filter from 49.5 to 50.5 Hz.

To assess the effects of the presentation of the gratings on gamma power (40-80 Hz) in sensor space, a time-frequency analysis was performed using a FFT approach with sliding time windows. We applied a fixed time window of 0.5 s and four orthogonal Slepian tapers resulting in ±5 Hz smoothing (34). Spectral power was then computed as the average across trials and tapers and was presented relative to baseline (−1 to −0.5 s).

Statistical analysis was performed on both sensor and source level (see following), using the same cluster-based randomization procedure (35). By clustering neighboring sensors (or grid points in the source analysis) that show the same effect, this test deals with the multiple-comparisons problem and, at the same time, takes into account the dependency of the data.

We applied a linearly constrained minimum variance beamformer technique to extract source-reconstructed gamma peak frequency and amplitude from the occipital lobe. Using the individual anatomical MRI, we constructed a realistically shaped single-shell description of the brain for each subject. The brain volume was divided into a grid with a 1-cm resolution and normalized to the template Montreal Neurological Institute brain, using SPM8 (www.fil.ion.ucl.ac.uk/spm). Lead fields were calculated for all grid points (36). We calculated the covariance matrix between all sensor pairs of the averaged band-passed (40–80 Hz) single trials and computed spatial filters for each subject, which were applied to reconstruct the raw time series as a virtual channel for the region of interest. Fourier spectra for the gamma range (40–80 Hz) were obtained with an FFT, using 9 Slepian multitapers (±5 Hz spectral smoothing) applied to 1-s data segments for the baseline time window (−1.0 to 0 s) and the time window of interest (0.5–1.5 s and 1.0–2.0 s stimulus presentation). Spectra were plotted relative to baseline and peak frequency and amplitude information extracted.

In addition, we used an adaptive algorithm fitting a Gaussian curve to the power spectra and used these for estimating the individual gamma peak frequency to confirm our original peak detection. This approach may give more accurate peak estimates (e.g., in case the spectrum contains two local maxima close to each other in the gamma range or in case of noisy spectra with spurious peaks), as it effectively smoothes the spectra. Furthermore, it is a more conservative approach, as subjects without substantial modulation in the gamma range are automatically omitted (Gaussian fit fails), allowing us to verify that our initial analysis was not biased by inclusion of potentially spurious peaks. For seven subjects, no clear peak could be fitted, and therefore these subjects were excluded from further analyses.

Regions of interest were generated in two ways. To assess the relationship of GABA and glutamate with gamma in the same location in the brain, we

took the Montreal Neurological Institute coordinates of the MRS voxel of each individual subject and used them as a spatial mask to extract gamma amplitude and frequency data. Furthermore, we determined the spatial distribution of power within the gamma band (40–80 Hz) in occipital cortex. A sphere of 17.5-mm radius was drawn around the peak of the activation and used as a spatial mask to extract frequency and amplitude. Because a previous study reporting a correlation between gamma peak frequency and GABA only presented gratings in the left visual field (9), we also specifically analyzed activity generated by the left and right gratings separately. Amplitude was expressed as percentage change from baseline.

MRS Methods. For MR data acquisition, a 3T Siemens scanner with a 32-channel head coil was used. A high-resolution T1-weighted anatomical image was acquired for each subject. The parameters were 224 slices (1 mm thick; distance factor = 50%, fov(read) = 256 mm, fov(phase) = 68.8%, matrix = 174 × 192, TR = 3000 ms, TE = 4.8 ms, TI = 1100 ms, flip angle = 8°, 1 concatenation, bandwidth = 220 Hz, echo spacing = 9.6 ms). Sagittal and axial T1 scout images were acquired and used to place a $2 \times 2 \times 2$ cm^3 voxel of interest manually in the occipital cortex (Fig. 1).

The SPECIAL sequence, originally developed by Mlynárik and colleagues (13) and adapted for humans by Mekle and colleagues (14), localized the single-voxel spectroscopy measurements. This sequence employs a very short echo-time acquisition, thereby minimizing signal loss resulting from T2 decay and scalar coupling. Although conventional short TE MRS is typically performed using a stimulated-echo approach, the SPECIAL sequence uses a spin-echo approach, which yields a factor two improvement in signal-to-noise ratio. Volumes were acquired using the following scan parameters: VOI = $2 \times 2 \times 2$ cm^3, TR/TE = 3,000 ms/8.5 ms, spectral width = 2 kHz, number of averages = 192, vector size = 2,048. Water suppression was achieved using the VAPOR method, which uses frequency selective pulses to suppress the water signal before excitation. Data acquisition could not be completed for one participant because of peripheral nerve stimulation.

For the MRS data analysis, before spectral analysis, eddy-current correction was applied to each water-suppressed spectrum, using the corresponding water-unsuppressed spectrum as an eddy-current reference. The spectra were then quantitatively analyzed, using a linear combination model. This analyzes the in vivo spectrum as a linear combination of a basis set of simulated metabolite spectra (15), as can be seen in Fig. 1. Simulated metabolite basis spectra were generated using an in-house Matlab-based implementation of the density matrix formalism, as described previously (18). All metabolite chemical shifts and coupling constants were taken from Govindaraju and colleagues (37). This way, we obtained a quantitative estimate for the concentration of each metabolite in arbitrary units, as well as its estimated uncertainty (Cramer-Rao lower bound). Given our interest in GABA and glutamate, we extracted the estimated concentrations for these neurotransmitters. There were no scans for which the uncertainty was more than 20% or peak line width was more than 8 Hz. Furthermore, we extracted levels of creatine, which is a measure of cellular integrity and the standard reference resonance (38). We then normalized our GABA and glutamate values by dividing them by creatine levels.

ACKNOWLEDGMENTS. We thank Steven Knight for assistance with data acquisition. This research was funded by Wellcome Trust studentships (to H.C. and G.W.), an Equipment Grant from the Wellcome Trust (092753/Z/10/Z), the National Institute for Health Research Oxford Biomedical Research Centre based at Oxford University Hospitals Trust Oxford University, and a Medical Research Council UK MEG Partnership Grant (MR/K005464/1). S.H. is funded by a Rubicon grant from the Netherlands Organization for Scientific Research.

1. Fries P (2009) Neuronal gamma-band synchronization as a fundamental process in cortical computation. *Annu Rev Neurosci* 32:209–224.
2. Buzsáki G, Wang XJ (2012) Mechanisms of gamma oscillations. *Annu Rev Neurosci* 35: 203–225.
3. Wang XJ (2010) Neurophysiological and computational principles of cortical rhythms in cognition. *Physiol Rev* 90(3):1195–1268.
4. Bartos M, Vida I, Jonas P (2007) Synaptic mechanisms of synchronized gamma oscillations in inhibitory interneuron networks. *Nat Rev Neurosci* 8(1):45–56.
5. Traub RD, Whittington MA, Stanford IM, Jefferys JG (1996) A mechanism for generation of long-range synchronous fast oscillations in the cortex. *Nature* 383(6601): 621–624.
6. Wang XJ, Buzsáki G (1996) Gamma oscillation by synaptic inhibition in a hippocampal interneuronal network model. *J Neurosci* 16(20):6402–6413.
7. Brunel N, Wang XJ (2003) What determines the frequency of fast network oscillations with irregular neural discharges? I. Synaptic dynamics and excitation-inhibition balance. *J Neurophysiol* 90(1):415–430.
8. Tiesinga P, Sejnowski TJ (2009) Cortical enlightenment: Are attentional gamma oscillations driven by ING or PING? *Neuron* 63(6):727–732.
9. Muthukumaraswamy SD, Edden RA, Jones DK, Swettenham JB, Singh KD (2009) Resting GABA concentration predicts peak gamma frequency and fMRI amplitude in response to visual stimulation in humans. *Proc Natl Acad Sci USA* 106(20):8356–8361.
10. Stagg CJ, Bachtiar V, Johansen-Berg H (2011) What are we measuring with GABA magnetic resonance spectroscopy? *Commun Integr Biol* 4(5):573–575.
11. Edden RA, Muthukumaraswamy SD, Freeman TC, Singh KD (2009) Orientation discrimination performance is predicted by GABA concentration and gamma oscillation frequency in human primary visual cortex. *J Neurosci* 29(50):15721–15726.
12. Gaetz W, Edgar JC, Wang DJ, Roberts TP (2011) Relating MEG measured motor cortical oscillations to resting γ-aminobutyric acid (GABA) concentration. *Neuroimage* 55(2):616–621.
13. Mlynárik V, Gambarota G, Frenkel H, Gruetter R (2006) Localized short-echo-time proton MR spectroscopy with full signal-intensity acquisition. *Magn Reson Med* 56(5): 965–970.
14. Mekle R, et al. (2009) MR spectroscopy of the human brain with enhanced signal intensity at ultrashort echo times on a clinical platform at 3T and 7T. *Magn Reson Med* 61(6):1279–1285.
15. Provencher SW (1993) Estimation of metabolite concentrations from localized in vivo proton NMR spectra. *Magn Reson Med* 30(6):672–679.
16. Wetzels R, Wagenmakers EJ (2012) A default Bayesian hypothesis test for correlations and partial correlations. *Psychon Bull Rev* 19(6):1057–1064.
17. Dienes Z (2011) Bayesian Versus Orthodox Statistics: Which Side Are You On? *Perspect Psychol Sci* 6:274–290.
18. Near J, Simpson R, Cowen P, Jezzard P (2011) Efficient γ-aminobutyric acid editing at 3T without macromolecule contamination: MEGA-SPECIAL. *NMR Biomed* 24(10): 1277–1285.
19. Near J, et al. (2013) Unedited in vivo detection and quantification of γ-aminobutyric acid in the occipital cortex using short-TE MRS at 3 T. *NMR Biomed* 26(11):1353–1362.
20. Stagg CJ, et al. (2011) Relationship between physiological measures of excitability and levels of glutamate and GABA in the human motor cortex. *J Physiol* 589(Pt 23): 5845–5855.
21. Jocham G, Hunt LT, Near J, Behrens TE (2012) A mechanism for value-guided choice based on the excitation-inhibition balance in prefrontal cortex. *Nat Neurosci* 15(7): 960–961.
22. Maddock RJ, Buonocore MH (2012) MR Spectroscopic Studies of the Brain in Psychiatric Disorders. *Curr Top Behav Neurosci*, 10.1007/7854_2011_197.
23. Tremblay S, et al. (2013) Relationship between transcranial magnetic stimulation measures of intracortical inhibition and spectroscopy measures of GABA and glutamate+glutamine. *J Neurophysiol* 109(5):1343–1349.
24. Hall SD, Barnes GR, Furlong PL, Seri S, Hillebrand A (2010) Neuronal network pharmacodynamics of GABAergic modulation in the human cortex determined using pharmaco-magnetoencephalography. *Hum Brain Mapp* 31(4):581–594.
25. Hall SD, et al. (2011) The role of GABAergic modulation in motor function related neuronal network activity. *Neuroimage* 56(3):1506–1510.
26. Muthukumaraswamy SD, et al. (2013) Elevating endogenous GABA levels with GAT-1 blockade modulates evoked but not induced responses in human visual cortex. *Neuropsychopharmacology* 38(6):1105–1112.
27. Saxena N, et al. (2013) Enhanced stimulus-induced gamma activity in humans during propofol-induced sedation. *PLoS ONE* 8(3):e57685.
28. Shaw A, et al. (2013) Marked reductions in visual evoked responses but not γ-aminobutyric acid concentrations or γ-band measures in remitted depression. *Biol Psychiatry* 73(7):691–698.
29. Hoogenboom N, Schoffelen JM, Oostenveld R, Parkes LM, Fries P (2006) Localizing human visual gamma-band activity in frequency, time and space. *Neuroimage* 29(3): 764–773.
30. Swettenham JB, Muthukumaraswamy SD, Singh KD (2009) Spectral properties of induced and evoked gamma oscillations in human early visual cortex to moving and stationary stimuli. *J Neurophysiol* 102(2):1241–1253.
31. Muthukumaraswamy SD, Singh KD, Swettenham JB, Jones DK (2010) Visual gamma oscillations and evoked responses: Variability, repeatability and structural MRI correlates. *Neuroimage* 49(4):3349–3357.
32. Oostenveld R, Fries P, Maris E, Schoffelen JM (2011) FieldTrip: Open source software for advanced analysis of MEG, EEG, and invasive electrophysiological data. *Comput Intell Neurosci* 2011:156869.
33. Jung TP, et al. (2000) Removal of eye activity artifacts from visual event-related potentials in normal and clinical subjects. *Clin Neurophysiol* 111(10):1745–1758.
34. Percival DB, Walden AT (1993) Spectral Analysis for Physical Applications: Multitaper and Conventional Univariate Techniques (Cambridge Univ Press, Cambridge, UK) pp XXVII, 583 S.
35. Maris E, Oostenveld R (2007) Nonparametric statistical testing of EEG- and MEG-data. *J Neurosci Methods* 164(1):177–190.
36. Nolte G (2003) The magnetic lead field theorem in the quasi-static approximation and its use for magnetoencephalography forward calculation in realistic volume conductors. *Phys Med Biol* 48(22):3637–3652.
37. Govindaraju V, Young K, Maudsley AA (2000) Proton NMR chemical shifts and coupling constants for brain metabolites. *NMR Biomed* 13(3):129–153.
38. Stagg CJ, et al. (2009) Polarity-sensitive modulation of cortical neurotransmitters by transcranial stimulation. *J Neurosci* 29(16):5202–5206.